JOURNAL OF AGRICULTURAL AND FOOD CHEMISTRY

Article

pubs.acs.org/JAFC

Borrelidin, a Potent Antifungal Agent: Insight into the Antifungal Mechanism against *Phytophthora sojae*

Ya-Mei Gao,[†,‡] Xiang-Jing Wang,[†] Ji Zhang,[†] Ming Li,[†] Chong-Xi Liu,[†] Jing An,[†] Ling Jiang,[†] and Wen-Sheng Xiang*[,†]

[†]School of Life Science, Northeast Agricultural University, Harbin 150030, People's Republic of China

[‡]College of Life Science and Technology, Heilongjiang Bayi Agricultural University, Daqing 163319, People's Republic of China

ABSTRACT: Borrelidin has high and specific antifungal activity against *Phytophthora sojae*. To explore the antifungal mechanism of borrelidin against *P. sojae*, the relationship between the antifungal activity of borrelidin and the concentration of threonine was evaluated. The results demonstrated that the growth-inhibitory effect of borrelidin on the growth of *P. sojae* was antagonized by threonine in a dose-dependent manner, suggesting that threonyl-tRNA synthetase (ThrRS) may be the potential target of borrelidin. Subsequently, the inhibition of the enzymatic activity of ThrRS by borrelidin *in vitro* was confirmed. Furthermore, the detailed interaction between ThrRS and borrelidin was investigated using fluorescence spectroscopy and circular dichroism (CD), implying a tight binding of borrelidin to ThrRS. Taken together, these results suggest that the antifungal activity of borrelidin against *P. sojae* was mediated by inhibition of ThrRS via the formation of the ThrRS−borrelidin complex.

KEYWORDS: *Borrelidin, Phytophthora sojae, antifungal activity, threonyl-tRNA synthetase*

INTRODUCTION

Borrelidin (Figure 1), an 18-membered macrolide polyketide produced by *Streptomyces* spp., exhibits a wide spectrum of

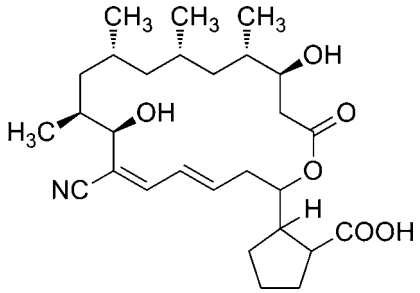

Figure 1. Structure of borrelidin.

biological activities, such as antibacterial activity,[1] antiviral activity,[2] anti-angiogenesis,[3,4] antimalarial activity,[5,6] and insecticidal and herbicidal activities.[7] Moreover, borrelidin also shows *in vitro* antifungal activity against phytopathogenic fungi and *Pythium* species with low EC_{50} values, which were in the range of 0.01−0.1 mg/L.[8] Especially, in our attempts to search for potent agricultural antibiotics, we found that borrelidin has high antifungal activity against dominant race 1 of *Phytophthora sojae* with an EC_{50} value of 0.0056 mg/L, which was at least 20-fold lower than those of the antifungal activity of borrelidin against other phytopathogenic fungi.[9] The effective antifungal activity of borrelidin implies its potency to be developed as a new antifungal agent against *P. sojae*. Therefore, it is imperative to further understand the antifungal mechanism of borrelidin against *P. sojae*. The reported biological activities of borrelidin are mainly associated with the specific inhibition of threonyl-tRNA synthetase (ThrRS) (EC 6.1.1.3) caused by borrelidin, leading to the disruption of protein synthesis.[10−13] However, the antifungal mechanism of borrelidin is still ambiguous.

Because of the high antifungal activitity of borrelidin as a potential new antifungal agent, the antifungal mechanism of borrelidin was explored in this study. Previous reports suggested that the involvement of ThrRS inhibition could be established using media containing a range of threonine concentrations.[14,15] Therefore, we examined the effect of threonine on the antifungal activity of borrelidin against *P. sojae* to confirm whether ThrRS was involved in the antifungal activity of borrelidin against *P. sojae*. Moreover, the ThrRS of *P. sojae* was overexpressed in *Escherichia coli*, and its sensitivity to borrelidin was evaluated. Furthermore, the interaction between *P. sojae* ThrRS and borrelidin was investigated by fluorescence spectroscopy. The binding properties, such as the quenching mechanism, the number of binding sites per protein, the binding force, and the binding distance, were obtained. The conformational change of ThrRS in the presence of borrelidin was also investigated by circular dichroism (CD) techniques. These studies provide insight into the antifungal mechanism of borrelidin and its potential for developing a novel agricultural antifungal agent against *Phytophthora* species.

MATERIALS AND METHODS

Reagents. Borrelidin was isolated from *Streptomyces* sp. neau-D50 with a purity of >95%, as previously described,[9] and was dissolved in methanol or dimethyl sulfoxide. Oligonucleotide synthesis and DNA sequencing were performed by Invitrogen. Nickel−nitrilotriacetic

Received: July 3, 2012
Revised: September 11, 2012
Accepted: September 12, 2012
Published: September 12, 2012

acid−agarose for His_6-tagged protein purification was from Qiagen (Qiagen, Inc., Valencia, CA). PrimerSTAR HS DNA polymerase, *Nde* I, and *Hind* III were all purchased from Takara (Takara Biotechnology Co., Ltd., Dalian, China). Threonine and *o*-phthaldehyde (OPA) were purchased from Sigma (Sigma-Aldrich (Shanghai) Trading Co, Ltd., Shanghai, China). *N*-Acetyl-L-cysteine was obtained from Aladdin (Aladdin Chemistry Co., Ltd., Shanghai, China). Other materials were of analytical reagent grade, and distilled water was used throughout the experiments.

Biological Material. *P. sojae* race 1 was kindly provided by the Soybean Research Institute of Northeast Agricultural University (Harbin, China) and cultured on carrot agar (CA) medium (carrot infusion from 200 g/L and 20 g/L agar) in the dark at 28 °C. The isolate has been deposited in the China General Microbiological Culture Collection Center (CGMCC 3.14914).

Effect of Threonine on the Antifungal Activity of Borrelidin against *P. sojae*. Petri dishes (9 cm diameter) containing 20 mL of CA medium were used for the antifungal activity assay. Borrelidin dissolved in methanol was serially diluted and added to CA to final concentrations of 0.006, 0.008, and 0.04 μg/mL, respectively. Then, threonine was added to each borrelidin containing CA to final concentrations of 0, 0.2, 0.4, and 0.6 mM. An agar plug of each fungal inoculum (6 mm diameter) was placed upside down in the center of each Petri dish. Methanol was used as a negative control. Three replicates were conducted for each treatment and incubated at 28 °C for 6−8 days in the dark, until the growth in the control plates reached the edges of the plates. Growth inhibition of the fungal strain was calculated as the percentage of inhibition of radial growth relative to the control. Inhibition (%) = {1 − [radial growth of treatment (mm)/radial growth of control (mm)]} × 100. Other amino acids, alamine, glutamine, tyrosine, and L-asparagine, were all tested using the same method.

Cloning and Expression of His_6-Tagged *P. sojae* ThrRS in *E. coli*. Genomic DNA of mycelia from *P. sojae* was extracted from fresh mycelia as described by Zelaya-Molina et al.[16] The cytosolic ThrRS of *P. sojae* was amplified by polymerase chain reaction (PCR). Two pairs of primers P1R/P1F and PR/PF were designed to obtain the *ThrRS* gene on the basis of the genome sequence of *P. sojae* strain P6497 and construct expression vector, respectively.[17] P1R and P1F primers were 5′-CCAGGTACACCCGCTGTGCGATCCAGTC-3′ and 5′-CGCAAATCGAGTCAAACTCACAACACTATCCT-3′. PF and PR primers flanking restriction sites (*Nde* I and *Hind* III) were 5′-GGAATTCCATATGAGCAGYGARCCCGCGCG-3′ and 5′-CCCAAGCTTCTCGTCGGCAGCCTTGGTCTC-3′. The PCR products were purified using a QIAquick PCR purification kit (Qiagen) according to the instructions of the manufacturer, cloned into the pET-32a (+) expression vectors using the *Nde* I and *Hind* III sites, and sequenced. The sequence was submitted to the National Center for Biotechnology Information (NCBI) (accession number JF727824). The plasmid pET32a-psThrRS-Htag, which encodes the enzyme with a C-terminal hexahistidine tag, was transformed into *E. coli* BL21 (Codonplus DE3) cells. The expression of psThrRS-Htag was continuously induced with 1 mM 1-thio-β-D-galactopyranoside for 20 h at 16 °C. *P. sojae* ThrRS protein were purified by nickel−nitrilotriacetic acid−agarose chromatography to ≥95% purity as judged by sodium dodecyl sulfate−polyacrylamide gel electrophoresis (SDS−PAGE) after Coomassie Brilliant Blue staining.[18] Pure ThrRS was dialyzed into 20 mM phosphate-buffered saline (PBS) or buffer A (20 mM Tris-HCl at pH 7.5, 15 mM $MgCl_2$, 150 mM KCl, and 1 mM β-mercaptoethanol), and then protein concentrations were determined by measurement at 280 nm using extinction coefficients by the method from Gill and von Hippel of 178 540 M^{-1} cm^{-1}. The enzyme was stored at −80 °C prior to use in experiments.

Borrelidin Inhibition of *P. sojae* ThrRS at the Step of Threonine Activation *in Vitro*. The borrelidin inhibition of *P. sojae* ThrRS at the step of threonine activation was measured. Enzymatic assay mixtures consisted of 10 mM $MgCl_2$, 30 mM KCl, 1 mM β-mercaptoethanol, 1 mM ATP, 0−20 μM borrelidin, and 4 μM enzyme and dissolved in 60 mM Tris-HCl (pH 7.5) (total volume of 0.2 mL). The enzymatic assay mixtures were preincubated for 10 min, and then threonine was added to initiate the reaction. Reactions were carried out in triplicate at 28 °C for 30 min. To determine the amount of free threonine, the reaction mixtures (0.2 mL) were incubated with 50 μL nickel−nitrilotriacetic acid−agarose for 10 min and centrifuged at 500*g* for 1 min to remove the ThrRS·Thr∼AMP complex. Then, 100 μL of supernatant was mixed with *o*-phthalaldehyde (OPA) standard solution for exactly 3 min of incubation according to McKerrow et al.,[19] and 20 μL aliquots were analyzed by high-performance liquid chromatography (HPLC). HPLC was carried out on Agilent 1100 Series (Agilent Technologies, Inc., Palo Alto, CA) at 25 °C with an eluent of acetonitrile/phosphate buffer [15:85 (v/v), 0.05 mol/L, pH 7.2] at a flow rate of 0.4 mL/min. The column used was a 4.6 × 250 mm inner diameter, 5 μm, TC-C18(2) silica column (Agilent Technologies, Inc., Palo Alto, CA). The detection was performed by an Agilent G1321A fluorescence detector with 365 nm excitation and 455 nm long-pass emission filters. The percentage of inhibition was calculated from the ratio of the initial velocity of the threonine activation in the presence of borrelidin (V_i) to that of the threonine activation in the absence of borrelidin (V_0). V_i/V_0 was plotted against the borrelidin concentration to obtain IC_{50} values. The apparent inhibition constant $K_i^{(app)}$ values were calculated on the basis of the simplified equation ($K_i^{(app)} = IC_{50} - [E]/2$, where $[E]$ represents the ThrRS concentration used in the experiment) derived for non-competitive tight binding inhibition.[20]

Fluorescence Measurements. Fluorescence measurements were performed on a model Hitachi F-7000 fluorescence spectrophotometer (Hitachi High Technologies, Tokyo, Japan) equipped with a personal computer (PC) and a thermostatic bath with an accuracy of ±0.1 °C. A total of 800 μL of enzyme and borrelidin solution was added accurately to the 5.0 mm quartz cell for fluorescence measurement. The concentration of enzyme was fixed at 0.25×10^{-6} M, while that of drug was varied in the range of $0-200 \times 10^{-6}$ M. The solution was first incubated at 27, 37, and 47 °C for 30 min, then the fluorescence spectra were measured with the width of the excitation and emission slit both adjusted at 5.0 nm. The excitation wavelength was 275 nm, and the emission spectrum was recorded from 280 to 500 nm. The scan speed was 2400 nm/min. The photomultiplier tube (PMT) voltage was 450 V.

CD Measurements. CD measurements were performed at 0.2 nm intervals with a MOS-450 spectrometer from BioLogic (BioLogic Science Instruments, Claix, France) using a 0.1 mm quartz cell. Acquisition duration was 5 s, with a slit of 2 nm. The readings of the blanks, which included the appropriate solvents, were subtracted from the readings of the sample solutions. CD spectra of protein (2 μM) were recorded in the range of 200−250 nm in the presence and absence of drug at 25 °C with 1 nm step size. The molar ratio of protein/drug was 1:1 and 1:5. The secondary structure was predicted on k2d3.[21]

RESULTS AND DISCUSSION

Effect of Threonine on Antifungal Activity of Borrelidin against *P. sojae*. It has been reported that bacterial and eukaryal ThrRS are specifically inhibited by borrelidin.[10−13] Because of the fact that the expression of ThrRS is regulated via a feedback mechanism,[22] the involvement of ThrRS inhibition could be tested using media containing a range of threonine concentrations.[14] Therefore, the media supplemented with threonine were employed to test whether ThrRS is involved in the antifungal activity of borrelidin against *P. sojae* and investigate the effects of threonine on antifungal activity of borrelidin against *P. sojae*. The results showed that the growth inhibition of *P. sojae* caused by borrelidin could be attenuated by threonine in a dose-dependent manner and the growth-inhibitory effect of borrelidin (0.006 μg/mL) on *P. sojae* could be completely suppressed at a concentration of 0.6 mM threonine (Figure 2). Furthermore, the attenuation in a dose-dependent manner was

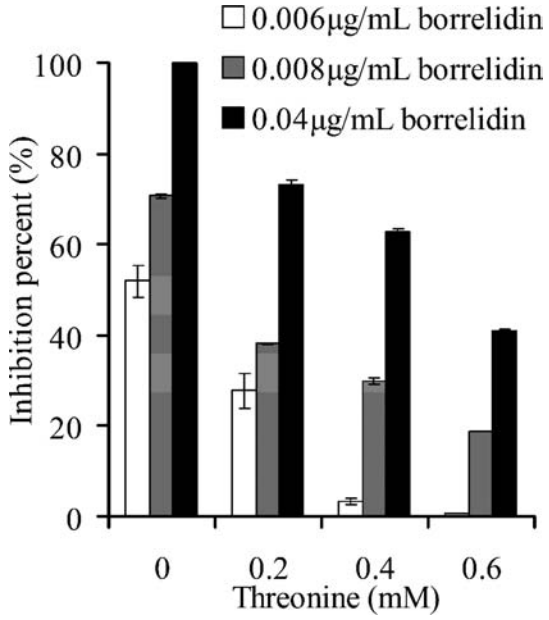

Figure 2. Effect of threonine on the antifungal activity of borrelidin against *P. sojae*.

specific for threonine, and other amino acids, such as alamine, glutamine, tyrosine, and L-asparagine, did not influence the inhibitory effect of borrelidin (Figure 3). These results clearly indicated the involvement of ThrRS in the antifungal activity of borrelidin against *P. sojae*.

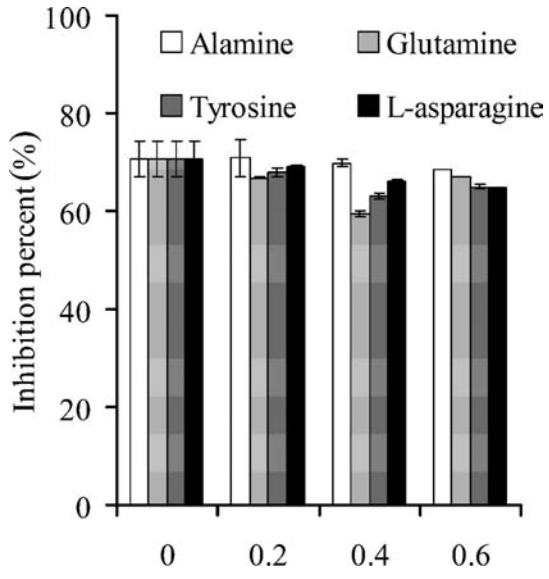

Figure 3. Effect of amino acids, alamine (A), glutamine (Q), tyrosine (Y), and L-asparagine (N), on the antifungal activity of borrelidin (0.008 μg/mL) against *P. sojae*.

Borrelidin Inhibits *P. sojae* ThrRS at the Step of Threonine Activation. To further investigate the *in vitro* inhibition of *P. sojae* ThrRS associated with borrelidin, the cytosolic *P. sojae* ThrRS was expressed in *E. coli* BL21 (Codonplus DE3) at a low temperature (16 °C) and purified from the cell supernatant using nickel–nitrilotriacetic acid–agarose chromatography (Figure 4).

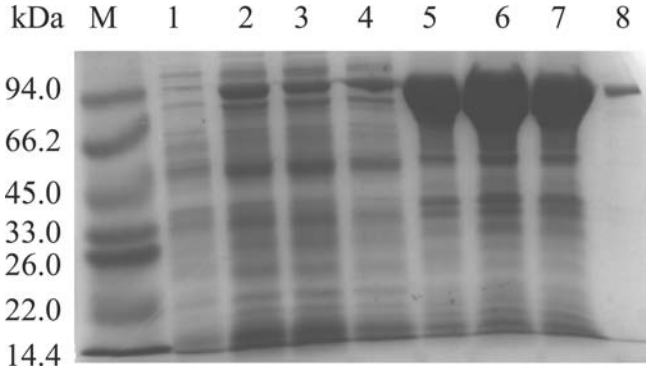

Figure 4. SDS–PAGE analysis of the recombinant *P. sojae* ThrRS. Lane M, protein molecular weight marker; lane 1, crude extract of an induced transformant harboring the empty plasmid pET-32a (+); lanes 2–4, debris of transformant *E. coli* BL21/pET-32a-psThrRS cells lysate; lanes 5–7, culture supernatant of transformant *E. coli* BL21/pET-32a-psThrRS cells lysate; and lane 8, purified psThrRS after Ni-affinity chromatography.

ThrRS catalyzes Thr-tRNA^{Thr} formation in two steps.[23] At the first step, it activates threonine to form the adenylate (Thr-AMP), and then it transfers the activated amino acid onto tRNA^{Thr} to generate Thr-tRNA^{Thr}. Borrelidin was believed to inhibit ThrRS at the first step of Thr-tRNA^{Thr} formation in *E. coli*;[24] therefore, the IC_{50} value for borrelidin inhibition of *P. sojae* ThrRS at the step of threonine activation was determined. When the concentration of *P. sojae* ThrRS was fixed at 4 μM, the IC_{50} value for borrelidin inhibition of *P. sojae* ThrRS at the step and $K_i^{(app)}$ were 8 μM (Figure 5) and 10 μM, respectively, which were close to the enzyme concentration (4 μM). This phenomenon was also observed in the experiment using *E. coli* ThrRS with a concentration of 1–2 nM as the target of

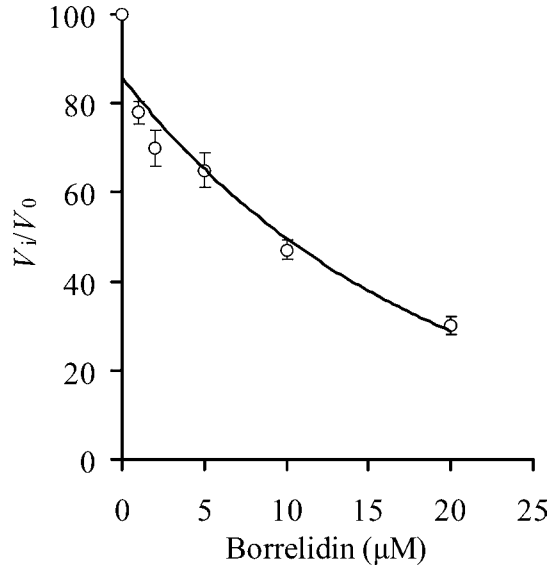

Figure 5. IC_{50} value of borrelidin inhibition on *P. sojae* ThrRS. Plot of the dose–response curve showing the percentage of initial velocity reduced by various amounts of borrelidin as measured in the first step of threonine activation by *P. sojae* ThrRS. The percentage of inhibition was calculated from the ratio of the initial velocity of the threonine activation in the presence of borrelidin to that in the absence of borrelidin. *P. sojae* ThrRS and threonine were 4 and 20 μM, respectively.

dx.doi.org/10.1021/jf302857x | J. Agric. Food Chem. 2012, 60, 9874–9881

borrelidin.[24] For the limits of detection in chromatography, borrelidin inhibition of ThrRS at the nanomole concentration was not measured. However, we speculated that $K_i^{(app)}$ and IC_{50} value for borrelidin inhibition of *P. sojae* ThrRS at the nanomole concentration would also be in the same order of magnitude, because of the fact that the IC_{50} value for borrelidin inhibition of ThrRS could vary remarkably depending upon the enzyme concentration and there was a linear dose−response curve of IC_{50} to the enzyme concentration at a fixed substrate concentration for *E. coli* ThrRS.[24] These results revealed that borrelidin can significantly inhibit the enzymatic activity, and therefore, the growth inhibition of *P. sojae* is probably caused by the decreased enzymatic activity of ThrRS associated with borrelidin.

Fluorescence Quenching of ThrRS by Borrelidin. The interaction of small molecules (e.g., drugs) with biological macromolecules is one of the most important phenomena in biophysical research[25−27] and has been studied extensively by many techniques, including fluorescence, infrared (IR), CD techniques, capillary electrophoresis, and molecular modeling.[28,29] To confirm the inhibition effect of borrelidin on *P. sojae* ThrRS and investigate the interaction between them, fluorescence spectroscopy was employed to study the binding property of borrelidin to *P. sojae* ThrRS.

The intrinsic fluorescence of proteins is mainly from tryptophan residues, and tryptophan is highly sensitive to the local environment. Each subunit of the ThrRS dimer of *P. sojae* possesses 10 tryptophan units distributed among the three principal structure domains. Fluorescence spectra depend upon the degree of exposure of the tryptophanyl side chain to the polar aqueous solvent and its proximity to specific quenching groups.[30] The protein concentration was fixed at 0.25×10^{-6} M, which has optical densities appropriated for the fluorescence quenching study. The fluorescence of the protein can be quenched in the concentration range of 20×10^{-6}−200×10^{-6} M borrelidin. The fluorescence spectra of ThrRS at a series of concentrations (0, 20×10^{-6}, 40×10^{-6}, 60×10^{-6}, 100×10^{-6}, and 200×10^{-6} M) of borrelidin at 27 °C are shown in Figure 6, which showed that ThrRS had a strong fluorescence emission peak (curve 1) at 332 nm after being excited with a wavelength of 275 nm. When borrelidin was titrated in the fixed concentration of ThrRS, the fluorescence intensity decreased significantly at three different temperatures. The results indicated that the fluorescence intensity of the 10 tryptophan residues of the protein was quenched by borrelidin and the microenvironment was changed after the addition of borrelidin.

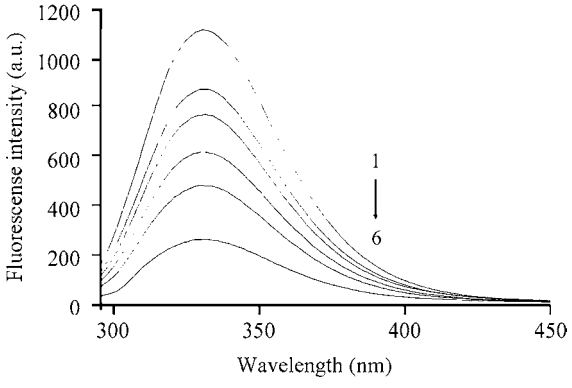

Figure 6. Fluorescence quenching spectra of *P. sojae* ThrRS (0.25×10^{-6} M) in the presence of increasing amounts of borrelidin following the excitation at 275 nm. (1−6) Indicate the emission spectra of protein in the presence of 0, 20×10^{-6}, 40×10^{-6}, 60×10^{-6}, 100×10^{-6}, and 200×10^{-6} M borrelidin. All data were obtained at 27 °C.

Mechanisms of Fluorescence Quenching of ThrRS by Borrelidin. Quenching can occur by different mechanisms, including dynamic quenching, static quenching, and both. Dynamic and static quenching can be distinguished by their different dependence upon the temperature of binding constants and viscosity or, preferably, by lifetime measurements.[31] Generally, the quenching constants decrease with an increasing temperature for static quenching, while the reverse is true for dynamic quenching.[31]

To investigate the quenching mechanism in the interaction between borrelidin and ThrRS, the fluorescence results obtained at 27, 37, and 47 °C were subjected to the Stern−Volmer equation

$$F_0/F = 1 + K_{SV}[Q] = 1 + k_q\tau_0[Q] \quad (1)$$

where F_0 and F are the fluorescence intensities of ThrRS in the absence and presence of borrelidin, respectively, K_{SV} is the Stern−Volmer quenching constant, k_q is the quenching rate constant of the biomolecule, τ_0 is the average lifetime of the biomolecule without the quencher ($\tau_0 = 10^{-8}$ s^{-1}),[32] and $[Q]$ is the concentration of the quencher.[31]

The Stern−Volmer plots of F_0/F versus $[Q]$ displayed a linear trend, which represent a single quenching mechanism, either static or dynamic. Figure 7 shows the Stern−Volmer plots of F_0/F versus $[Q]$ at the three temperatures, and the calculated quenching constants at the corresponding temperatures are listed in Table 1. The decreasing trend of K_{SV} with an increase in the temperature revealed the presence of the static quenching mechanism in the binding of borrelidin to ThrRS. The maximum scatter collision quenching constant of various quenchers with biopolymer is 2.0×10^{10} M^{-1} s^{-1}.[33] In this study, the values of the rate constant k_q (K_{SV}/τ_0) for the quenching of ThrRS caused by borrelidin is much larger than the maximum diffusion collision quenching rate constant for

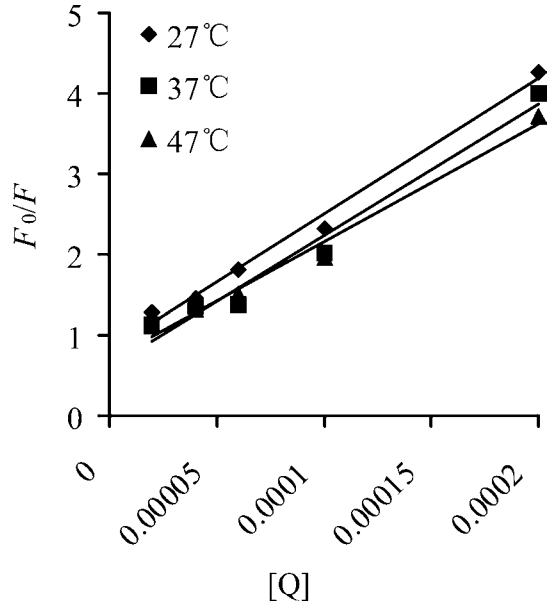

Figure 7. Stern−Volmer plots for borrelidin−ThrRS of *P. sojae* at three different temperatures. The concentration of ThrRS was 0.25×10^{-6} M.

Table 1. Stern–Volmer Quenching Constants for Borrelidin–ThrRS Systems at Different Temperatures

T (°C)	K_{SV} ($\times 10^4$, M^{-1})	k_q ($\times 10^{12}$, L mol^{-1} s^{-1})	R^2 [a]
27	1.542	1.542	0.9788
37	1.331	1.331	0.9201
47	1.233	1.233	0.9452

[a]Correlation coefficient.

the scatter mechanism. Hence, we proposed that the quenching is not initiated by dynamic collision but originates from the formation of a complex.[30,34]

Analysis of Binding Equilibria between ThrRS and Borrelidin. For the static quenching interaction, the binding constant, K_A, and the number of binding sites, n, can be calculated using the equation shown below[35]

$$\log[(F_0 - F)/F] = \log K_A + n \log[Q] \quad (2)$$

where F_0 and F are the fluorescence intensities of ThrRS without and with borrelidin, respectively, and $[Q]$ is the concentration of the quencher. From the linear plot of $\log(F_0 - F)/F$ versus $\log[Q]$, the values of K_A and n were obtained from the intercept and slope, 2.552×10^5 M^{-1} and 1.331, respectively. The values of n for borrelidin–ThrRS were approximately equal to 1, indicating one independent class of binding sites on dimeric ThrRS for borrelidin. The result is in agreement with the previous report, which showed that borrelidin appears to be stoichiometric with dimeric ThrRS.[24]

Thermodynamic Parameters and Binding Forces of the Interaction between ThrRS and Borrelidin. The interaction forces between borrelidin and ThrRS may be of four kinds: hydrophobic forces, hydrogen bonds, van der Waals forces, and electrostatic interactions.[36] The thermodynamic parameters, enthalpy change (ΔH), entropy change (ΔS), and free energy change (ΔG), are important to propose the binding mode.[37] ΔH can be calculated by the linear fitting plot of ln K versus $1/T$ based on the van't Hoff equation given below

$$\ln K = -\Delta H/RT + \Delta S/R \quad (3)$$

where R is the gas constant, T is the experimental temperature, and K is the binding constant at the corresponding T, respectively.[38]

The value of ΔG was calculated using the following equation based on the binding constants at different temperatures:

$$\Delta G = \Delta H - T\Delta S = -RT \ln K \quad (4)$$

The values of ΔG for the interaction of borrelidin with ThrRS at three different temperatures are all negative, and the negative values of ΔG revealed that the interaction process of borrelidin with ThrRS is spontaneous. According to the theory by Ross and Subramanian,[36] the positive enthalpy change (ΔH) and entropy change (ΔS) indicate the hydrophobic interaction. The negative values of ΔH and ΔS indicate hydrogen binding and van der Waals interactions, whereas the very low positive or negative enthalpy change ΔH and positive entropy change ΔS values are associated with electrostatic interactions. The values of ΔH (85.024 kJ/mol) and ΔS (0.372 kJ mol^{-1} K^{-1}) are both found to be positive, which indicates that the binding is mainly entropy-derived and the hydrophobic forces play a major role in the binding process of borrelidin to *P. sojae* ThrRS.

Fluorescence Resonance Energy Transfer (FRET) between ThrRS and Borrelidin. The distance between ThrRS and borrelidin was estimated by Förster's non-radiative energy transfer theory. The overlap of the fluorescence spectra of ThrRS and the ultraviolet–visible (UV–vis) absorption spectra of borrelidin is shown in Figure 8. The efficiency of

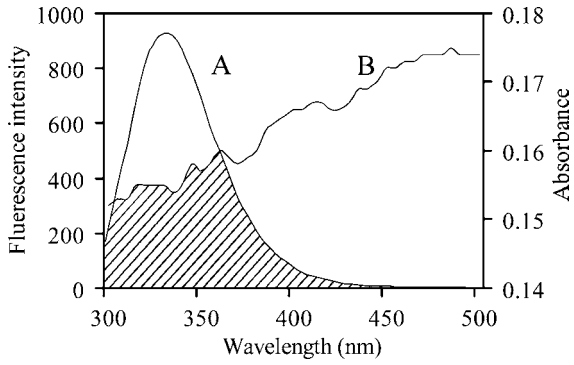

Figure 8. Spectral overlap between the fluorescence emission spectrum of (A) ThrRS and UV–vis absorption spectrum of (B) borrelidin at 24 °C. The concentration of ThrRS and borrelidin was 0.25×10^{-6} M.

energy transfer, E, was calculated according to Förster's energy-transfer theory

$$E = 1 - F/F_0 = R_0^6/(R_0^6 + r^6) \quad (5)$$

where F and F_0 are the fluorescence intensities of ThrRS in the presence and absence of borrelidin, r is the distance between the acceptor and donor, and R_0 is the critical distance when the transfer efficiency is 50%.[39] The value of R_0 was evaluated as follows:

$$R_0^6 = 8.8 \times 10^{-25} k^2 N^{-4} \Phi J \quad (6)$$

where k^2 is the spatial orientation factor of the dipole, N is the refractive index of the medium, Φ is the fluorescence quantum yield of the donor in the absence of the acceptor, and J expresses the degree of spectral overlap between the donor emission and the acceptor absorption. J is defined as

$$J = \sum F(\lambda)\varepsilon(\lambda)\lambda^4 \Delta\lambda / \sum F(\lambda)\Delta\lambda \quad (7)$$

where $F(\lambda)$ is the fluorescence intensity of the fluorescent donor of wavelength λ and $\varepsilon(\lambda)$ is the molar absorption coefficient of the acceptor at wavelength λ. In the present case, $k^2 = {}^2/_3$, $N = 1.336$, and $\Phi = 0.15$ for ThrRS. The following data were obtained: $J = 2.14 \times 10^{-15}$ cm^3 L mol^{-1}, $R_0 = 4.254$ nm, and $E = 0.079$. The binding distance r between borrelidin and *P. sojae* ThrRS is 6.39 nm. The donor–acceptor distance r is less than 7 nm, which indicates that the fluorescence quenching of ThrRS is also a non-radiation transfer process, and reveals the presence of static quenching in the interaction.

Conformational Changes of ThrRS in the Presence of Borrelidin. It has been ascertained that the binding of borrelidin to ThrRS can lead to the fluorescence quenching of ThrRS, but it is still a question as to whether the binding affects the conformation and/or microenvironment of ThrRS. Therefore, CD was employed to monitor the conformational changes of ThrRS protein in the presence of borrelidin. The CD spectra of *P. sojae* ThrRS exhibited two negative bands in the UV region at 208 and 220 nm, which are characteristic of the α-helicity of protein (Figure 9). When the ratio of borrelidin/protein was increased from 0 to 5, the β-sheet content was reduced from 25.6 to 21.8% and the α-helix

dx.doi.org/10.1021/jf302857x | J. Agric. Food Chem. 2012, 60, 9874–9881

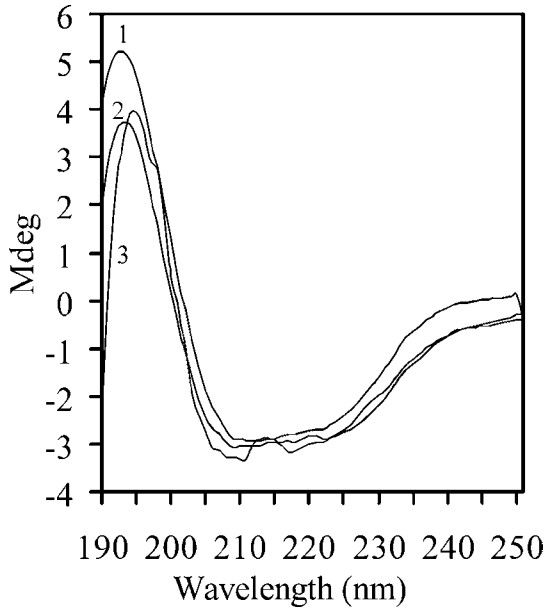

Figure 9. CD spectra of ThrRS (2 μM) of *P. sojae* in the (1) absence and presence of (2) 2 μM and (3) 10 μM borrelidin.

content was increased from 18.3 to 25.7% (Table 2). The results demonstrated that the binding of borrelidin could induce the conformational changes of ThrRS with an increased content of α-helicity and a decreased content of β-sheet. Conformational changes in ligand−receptor interactions were proven to be important for ligand binding with the receptor.[40−43] According to the Structural Classification of Proteins (SCOP) database, the folding of ThrRS is an α and β protein ($\alpha + \beta$). This folding topology includes β-sheets, which are mostly antiparallel. The α-helices and β-sheets are commonly segregated. The active site is surrounded on one side by antiparallel, β-sheets and α-helices on the opposite side.[44] CD results showed that the α-helicity and β-sheet of ThrRS both changed after the formation of the complex of ThrRS−borrelidin. We proposed that borrelidin binds in the catalytic region of ThrRS, which was consistent with the results predicted by Ruan et al.[24] However, we believe that the three-dimensional structure of the ThrRS and borrelidin complex will provide the key information for the inhibition mechanism of borrelidin to ThrRS in detail.

Table 2. Secondary Structural Analysis for the Native ThrRS and the Complex with Borrelidin

molar ratio of protein/borrelidin	α-helix (%)	β-sheet (%)
1:0	18.3	25.6
1:1	24.4	22.4
1:5	25.7	21.8

Although the function of aminoacyl-tRNA synthetases was conserved, they evolved into finely tuned structures with significant divergence among the three domains of the tree of life.[45] Finely tuned structural differences among aminoacyl-tRNA synthetase orthologues make the enzyme a promising target of species-specific inhibitors. For example, mupirocin selectively inhibits the prokaryotic isoleucyl-tRNA synthetases but has little or no effect on the eukaryotic enzymes.[46] Indolmycin inhibits only one of the two tryptophanyl-tRNA synthetases in *Streptomyces coelicolor*.[47] Therefore, it is possible to find an inhibitor as an agricultural agent that can selectively inhibit ThrRS. A unique hydrophobic cluster was predicted to contribute to differences in borrelidin inhibition among ThrRS, and this cluster is conserved in most organisms, except for archaea *Archaeoglobus fulgidus* and *Methanocaldococcus jannaschi* and pathogen *Helicobacter pylori*. We also performed the alignment of *P. sojae* ThrRS, archaeal, and eukaryotic ThrRS protein sequences to reveal the sequence conservation of the *P. sojae* ThrRS. The corresponding hydrophobic region (Ser-410, His-412, Cys-437, Pro-438, Leu-593, and Phe-597) was found with two conserved amino acid replacements compared to that in *E. coli*, which may explain why borrelidin possesses the high and selective antifungal activity against *P. sojae*. However, the influence of these conserved amino acid replacements in *P. sojae* ThrRS on the high antifungal activity of borrelidin against *P. sojae* remains to be investigated.

In conclusion, the mechanism of antifungal activity of borrelidin against *P. sojae* was investigated in this work. The effect of threonine on the antifungal activity of borrelidin against *P. sojae* and borrelidin inhibition of *P. sojae* ThrRS enzyme activity *in vitro* proved that borrelidin is an inhibitor of ThrRS. This work also reported the detailed interaction of borrelidin with ThrRS, indicating that the antifungal activity of borrelidin against *P. sojae* was mediated through the formation of the ThrRS−borrelidin complex. These results may be important for developing borrelidin as an effective antifungal agent.

AUTHOR INFORMATION

Corresponding Author

*Telephone/Fax: +86-451-55190413. E-mail: xiangwensheng@yahoo.com.cn.

Funding

This work was financially supported by the National Key Project for Basic Research (2010CB126102), the National Natural Science Foundation of China (305771427 and 31000884), the Special Fundation for Scientific and Technological Innovation Research of Harbin (Grant 2011RFXXN038), and the Natural Science Foundation of Heilongjiang Province (Grant C201029).

Notes

The authors declare no competing financial interest.

REFERENCES

(1) Berger, J.; Jampolsky, L. M.; Goldberg, M. W. Borrelidin, a new antibiotic with anti-borrelia activity and penicillin enhancement properties. *Arch. Biochem.* **1949**, *22*, 476−478.

(2) Dickinson, L.; Griffiths, A. J.; Mason, C. G.; Mills, R. F. Anti-viral activity of two antibiotics isolated from a species of *Streptomyces*. *Nature* **1965**, *206*, 265−268.

(3) Wakabayashi, T.; Kageyama, R.; Naruse, N.; Tsukahara, N.; Funahashi, Y.; Kitoh, K.; Watanabe, Y. Borrelidin is an angiogenesis inhibitor; disruption of angiogenic capillary vessels in a rat aorta matrix culture model. *J. Antibiot.* **1997**, *50*, 671−676.

(4) Habibi, D.; Ogloff, N.; Jalili, R. B.; Yost, A.; Weng, A. P.; Ghahary, A.; Ong, C. J. Borrelidin, a small molecule nitrile-containing macrolide inhibitor of threonyl-tRNA synthetase, is a potent inducer of apoptosis in acute lymphoblastic leukemia. *Invest. New Drugs* **2012**, *30*, 1361−1370.

(5) Otoguro, K.; Ui, H.; Ishiyama, A.; Kobayashi, M.; Togashi, H.; Takahashi, Y.; Masuma, R.; Tanaka, H.; Tomoda, H.; Yamada, H.; Omura, S. *In vitro* and *in vivo* antimalarial activities of a non-glycosidic 18-membered macrolide antibiotic, borrelidin, against drug-resistant strains of *Plasmodia*. *J. Antibiot.* **2003**, *56*, 727−729.

(6) Ishiyama, A.; Iwatsuki, M.; Namatame, M.; Nishihara-Tsukashima, A.; Sunazuka, T.; Takahashi, Y.; Ōmura, S.; Otoguro, K. Borrelidin, a potent antimalarial: Stage-specific inhibition profile of synchronized cultures of *Plasmodium falciparum*. *J. Antibiot.* **2011**, *64*, 381−384.
(7) Dorgrrloh, M.; Kretsehmer, A.; Schmidt, R. R.; Steffens, R.; Zoebelein, G.; Tietjen, K.; Roeben, W.; Stendel, W.; Saleher, O. Borreldin insecticide and herbicide and its preparation by fermentation. Ger. Offen. DE 3,607,287 A1, July 1, 1988.
(8) Shiang, M.; Kuo, M. Y.; Chu, K. C.; Chang, P. C.; Chang, H. Y.; Lee, H. P. Strain of *Streptomyces*, and relevant uses thereof. U.S. Patent 6,193,964 B1, 2001.
(9) Liu, C. X.; Zhang, J.; Wang, X. J.; Qian, P. T.; Wang, J. D.; Gao, Y. M.; Yan, Y. J.; Zhang, S. Z.; Xu, P. F.; Li, W. B.; Xiang, W. S. Antifungal activity of borrelidin produced by a *Streptomyces* strain isolated from soybean. *J. Agric. Food Chem.* **2012**, *60*, 1251−1257.
(10) Paetz, W.; Nass, G. Biochemical and immunological characterization of threonyl-tRNA synthetase of two borrelidin-resistant mutants of *Escherichia coli* K12. *Eur. J. Biochem.* **1973**, *35*, 331−337.
(11) Gerken, S. C.; Arfin, S. M. Chinese hamster ovary cells resistant to borrelidin overproduce threonyl-tRNA synthetase. *J. Biol. Chem.* **1984**, *259*, 9202−9206.
(12) Nass, G.; Poralla, K. Genetics of borrelidin resistant mutants of *Saccharomyces cerivisiae* and properties of their threonyl-tRNA-synthetase. *Mol. Gen. Genet.* **1976**, *147*, 39−43.
(13) Nass, G.; Hasenbank, R. Effect of borrelidin on the threonyl-tRNA-synthetase activity and the regulation of threonine-biosynthetic enzymes in *Saccharomyces cerivisiae*. *Mol. Gen. Genet.* **1970**, *108*, 28−32.
(14) Kawamura, T.; Liu, D.; Towle, M. J.; Kageyama, R.; Tsukahara, N.; Wakabayashi, T.; Littlefield, B. A. Anti-angiogenesis effects of borrelidin are mediated through distinct pathways: Threonyl-tRNA synthetase and caspases are independently involved in suppression of proliferation and induction of apoptosis in endothelial cells. *J. Antibiot.* **2003**, *56*, 709−715.
(15) Gantt, J. S.; Bennett, C. A.; Arfin, S. M. Increased levels of threonyl-tRNA synthetase in a borrelidin-resistant Chinese hamster ovary cell line. *Proc. Natl. Acad. Sci. U.S.A.* **1981**, *78*, 5367−5370.
(16) Zelaya-Molina, L. X.; Ortega, M. A.; Dorrance, A. E. Easy and efficient protocol for oomycete DNA extraction suitable for population genetic analysis. *Biotechnol. Lett.* **2011**, *33*, 715−720.
(17) Tyler, B. M.; Tripathy, S.; Zhang, X.; Dehal, P.; Jiang, R. H.; Aerts, A.; Arredondo, F. D.; Baxter, L.; Bensasson, D.; Beynon, J. L.; Chapman, J.; Damasceno, C. M.; Dorrance, A. E.; Dou, D.; Dickerman, A. W.; Dubchak, I. L.; Garbelotto, M.; Gijzen, M.; Gordon, S. G.; Govers, F.; Grunwald, N. J.; Huang, W.; Ivors, K. L.; Jones, R. W.; Kamoun, S.; Krampis, K.; Lamour, K. H.; Lee, M. K.; McDonald, W. H.; Medina, M.; Meijer, H. J.; Nordberg, E. K.; Maclean, D. J.; Ospina-Giraldo, M. D.; Morris, P. F.; Phuntumart, V.; Putnam, N. H.; Rash, S.; Rose, J. K.; Sakihama, Y.; Salamov, A. A.; Savidor, A.; Scheuring, C. F.; Smith, B. M.; Sobral, B. W.; Terry, A.; Torto-Alalibo, T. A.; Win, J.; Xu, Z.; Zhang, H.; Grigoriev, I. V.; Rokhsar, D. S.; Boore, J. L. *Phytophthora* genome sequences uncover evolutionary origins and mechanisms of pathogenesis. *Science* **2006**, *313*, 1217.
(18) Sambrook, J.; Fritsch, E. F.; Maniatis, T. Detection and analysis of proteins expressed from cloned genes. In *Molecular Cloning: A Laboratory Manual*, 2nd ed.; Cold Spring Harbor Press: New York, 1989; pp 18.47−18.59.
(19) McKerrow, J.; Vagg, S.; McKinney, T.; Seviour, E. M.; Maszenan, A. M.; Brooks, P.; Seviour, R. J. A simple HPLC method for analysing diaminopimelic acid diastereomers in cell walls of Gram-positive bacteria. *Lett. Appl. Microbiol.* **2000**, *30*, 178−182.
(20) Copeland, R. A. Tight binding inhibitors. In *Enzymes: A Practical Introduction to Structure, Mechanism, and Data Analysis*, 2nd ed.; Wiley-VHC: New York, 2000; pp 305−317.
(21) Louis-Jeune, C.; Andrade-Navarro., M. A.; Perez-Iratxeta, C. Prediction of protein secondary structure from circular dichroism using theoretically derived spectra. *Proteins* **2012**, *80*, 374−381.
(22) Freist, W.; Gauss, D. H. Threonyl-tRNA synthetase. *Biol. Chem. Hoppe-Seyler* **1995**, *376*, 213−224.
(23) Ibba, M.; Söll, D. The renaissance of aminoacyl-tRNA synthesis. *EMBO Rep.* **2001**, *2*, 382−387.
(24) Ruan, B.; Bovee, M. L.; Sacher, M.; Stathopoulos, C.; Poralla, K.; Francklyn, C. S.; Söll, D. A unique hydrophobic cluster near the active site contributes to differences in borrelidin inhibition among threonyl-tRNA synthetases. *J. Biol. Chem.* **2005**, *280*, 571−577.
(25) Zhang, J.; Wang, X. J.; Yan, Y. J.; Xiang, W. S. Comparative studies on the interaction of genistein, 8-chlorogenistein, and 3′,8-dichlorogenistein with bovine serum albumin. *J. Agric. Food Chem.* **2011**, *59*, 7506−7513.
(26) Kim, D.; Park, J.; Kim, J.; Han, C.; Yoon, J.; Kim, N.; Seo, J.; Lee, C. Flavonoids as mushroom tyrosinase inhibitors: A fluorescence quenching study. *J. Agric. Food Chem.* **2006**, *54*, 935−941.
(27) Cheng, F. Q.; Wang, Y. P.; Li, Z. P.; Dong, C. Fluorescence study on the interaction of human serum albumin with bromsulphalein. *Spectrochim. Acta., Part A* **2006**, *65*, 1144−1147.
(28) Nieto, M.; Perkins, H. R.; Frère, J. M.; Ghuysen, J. M. Fluorescence and circular dichroism studies on the *Streptomyces* R61 DD-carboxypeptidase-transpeptidase. Penicillin binding by the enzyme. *Biochem. J.* **1973**, *135*, 493−505.
(29) Ricci, G.; De Maria, F.; Antonini, G.; Turella, P.; Bullo, A.; Stella, L.; Filomeni, G.; Federici, G.; Caccuri, A. M. 7-Nitro-2,1,3-benzoxadiazole derivatives, a new class of suicide inhibitors for glutathione *S*-transferases. Mechanism of action of potential anticancer drugs. *J. Biol. Chem.* **2005**, *280*, 26397−26405.
(30) Qin, P.; Liu, R.; Pan, X.; Fang, X.; Mou, Y. Impact of carbon chain length on binding of perfluoroalkyl acids to bovine serum albumin determined by spectroscopic methods. *J. Agric. Food Chem.* **2010**, *58*, 5561−5567.
(31) Lakowicz, J. R. Quenching of fluorescence. In *Principles of Fluorescence Spectroscopy*, 2nd ed.; Plenum Press: New York, 1999; pp 237−265.
(32) Lakowica, J. R.; Weber, G. Quenching of fluorescence by oxygen. A probe for structural fluctuantions in macromolecules. *Biochemistry* **1973**, *12*, 4161−4170.
(33) Eftink, M. R.; Ghiron, C. A. Fluorescence quenching studies with proteins. *Anal. Biochem.* **1981**, *114*, 199−212.
(34) Chi, Z.; Liu, R.; Teng, Y.; Fang, X.; Gao, C. Binding of oxytetracycline to bovine serum albumin: Spectroscopic and molecular modeling investigations. *J. Agric. Food Chem.* **2010**, *58*, 10262−10269.
(35) Chipman, D. M.; Grisaro, V.; Sharon, N. The binding of oligosaccharides containing *N*-acetylglucosamine and *N*-acetylmuramic acid to lysozyme. *J. Biol. Chem.* **1967**, *242*, 4388−4394.
(36) Ross, P. D.; Subramanian, S. Thermodynamics of protein association reactions: Forces contributing to stability. *Biochemistry* **1981**, *20*, 3096−3102.
(37) Kandagal, P. B.; Ashoka, S.; Seetharamappa, J.; Shaikh, S. M. T.; Jadegoud, Y.; Ijare, O. B. Study of the interaction of an anticancer drug with human and bovine serum albumin: Spectroscopic approach. *J. Pharm. Biomed. Anal.* **2006**, *41*, 393−399.
(38) Haynie, D. T. Gibbs free energy-theory. In *Biological Thermodynamics*; Cambridge University Press: Cambridge, U.K., 2001; pp 73−117.
(39) Forster, T. Delocalized excitation and excitation transfer. In *Modern Quantum Chemistry*, Istanbul Lectures; Sinanoglu, O., Ed.; Academic Press, Inc.: New York, 1966; Section 3-B, pp 93−137.
(40) Hao, G. F.; Wang, F.; Li, H.; Zhu, X. L.; Yang, W. C.; Huang, L. S.; Wu, J. W.; Berry, E. A.; Yang, G. F. Computational discovery of picomolar Q_o site inhibitors of cytochrome bc_1 complex. *J. Am. Chem. Soc.* **2012**, *134*, 11168−11176.
(41) Hao, G. F.; Yang, G. F. The role of Phe82 and Phe351 in auxin-induced substrate perception by TIR1 ubiquitin ligase: A novel insight from molecular dynamics simulations. *PLoS One* **2010**, *5*, No. e10742.
(42) Zhao, P. L.; Wang, L.; Zhu, X. L.; Huang, X. Q.; Zhan, C. G.; Wu, J. W.; Yang, G. F. Subnanomolar inhibitor of cytochrome bc_1 complex designed by optimizing interaction with conformationally flexible residues. *J. Am. Chem. Soc.* **2010**, *132*, 185−194.

(43) Zhang, L.; Hao, G. F.; Tan, Y.; Xi, Z.; Huang, M. Z.; Yang, G. F. Bioactive conformation analysis of cyclic imides as protoporphyrinogen oxidase inhibitor by combining DFT calculations, QSAR and molecular dynamic simulations. *Bioorg. Med. Chem.* **2009**, *17*, 4935−4942.
(44) Ibba, M.; Francklyn, C.; Cusack, S. Threonyl-tRNA synthetase. In *The Aminoacyl-tRNA Synthetases*; Landes Bioscience: Georgetown, TX, 2005; pp 164−165.
(45) Wolf, Y. I.; Aravind, L.; Grishin, N. V.; Koonin, E. V. Evolution of aminoacyl-tRNA synthetases analysis of unique domain architectures and phylogenetic trees reveals a complex history of horizontal gene transfer events. *Genome Res.* **1999**, *9*, 689−710.
(46) Yanagisawa, T.; Lee, J. T.; Wu, H. C.; Kawakami, M. Relationship of protein structure of isoleucyl-tRNA synthetase with pseudomonic acid resistance of *Escherichia coli*. A proposed mode of action of pseudomonic acid as an inhibitor of isoleucyl-tRNA synthetase. *J. Biol. Chem.* **1994**, *269*, 24304−24309.
(47) Kitabatake, M.; Ali, K.; Demain, A.; Sakamoto, K.; Yokoyama, S.; Söll, D. Indolmycin resistance of *Streptomyces coelicolor* A3(2) by induced expression of one of its two tryptophanyl-tRNA synthetases. *J. Biol. Chem.* **2002**, *277*, 23882−23887.